THE JOURNAL OF PHYSICAL CHEMISTRY C

Article

Cite This: J. Phys. Chem. C 2018, 122, 13937−13943

pubs.acs.org/JPCC

# Competing Energy Transfer Pathways in a Five-Chromophore Perylene Array

Vineeth B. Yasarapudi,[†] Laszlo Frazer,[†,§] James E. A. Webb,[‡] Joseph K. Gallaher,[†] Alexander Macmillan,[¶] Alexander Falber,[‡] Pall Thordarson,[‡] and Timothy W. Schmidt*,[†]

[†]ARC Centre of Excellence in Exciton Science, School of Chemistry, UNSW Sydney, Sydney, NSW 2052, Australia

[‡]Australian Centre for Nanomedicine and the ARC Centre of Excellence in Bio-Nano Science & Technology, School of Chemistry, UNSW Sydney, Sydney, NSW 2052, Australia

[¶]Mark Wainwright Analytical Centre, UNSW Sydney, Sydney, NSW 2052, Australia

[§]ARC Centre of Excellence in Exciton Science, School of Chemistry, Monash University, Clayton, VIC 3800, Australia

Supporting Information

**ABSTRACT:** A perylene (donor−dimer)−acceptor−(donor−dimer) pentamer array is synthesized to investigate the competition between excimer formation and Förster resonance energy transfer. Using time-resolved fluorescence, we show that, upon excitation, the isolated perylene dimer forms an excimer with a time constant of 4.3 ns. However, in the pentamer array, when either of two constituent dimers donate their energy to the acceptor fluorophore, the excimer energy trap is eliminated. The pentamer macromolecule shows broad absorption and reduced self-absorption, at some cost to fluorescence quantum yield.

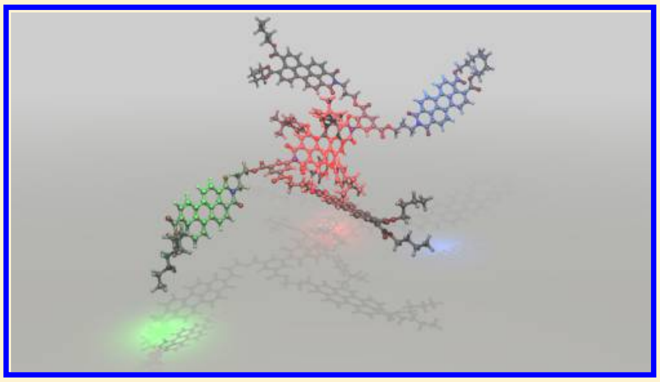

## INTRODUCTION

Global solar energy reserves are on the order of $10^{16}$ W, which dwarfs current consumption by 3 orders of magnitude.[1] Therefore, light-driven devices can be cheap to operate. The effectiveness of organic light- or electrically-driven devices designed to produce photocurrent, light, or chemical reactions depends on controlled generation and transport of excitons. The controlled transport of excitonic energy relies on the interactions between chromophores,[2] which may or not be covalently bonded.

In organic solar cells,[3] the photogenerated exciton must diffuse to the heterojunction. In organic light-emitting diodes the electrically generated exciton ideally migrates to a highly luminescent dopant.[4,5] Dendrimers can be useful for directing excitons to an active site which performs re-emission,[6−9] charge separation,[10] or a chemical reaction.[11] Photosystem II is an example where multiple chlorophylls sensitize reaction centers. In single molecule devices, absorption can be strengthened by covalently bonding more chromophores to the active component.[12]

When attaching a large number of chromophores to an active site, it is necessary that the chromophores are close. If two similar-energy chromophores are closely situated, even H-aggregated, and one is optically excited, they can form an excimer.[2,13−20] The excimer is often a detrimental energy trap, and usually exhibits a cancellation of radiative transition moments which could hinder subsequent Förster resonance energy transfer (FRET).[21] The competition between excimer formation and FRET is thus of relevance to a range of excitonic devices.

In this paper, we investigate the competition between excimer formation and FRET in a five-chromophore perylene array consisting of an acceptor and two donor dimers. The acceptor is a perylene diimide bay-functionalized with four phenoxyl groups. The donor chromophore is a perylene monoimide diester, shown in Scheme 1. These are ligated to form a dimer which readily forms an excimer.[22] The dimer is shown in Scheme 2.

Rather than attempting to separate the two parts of the dimer, we are interested in the competition between excimer formation and FRET, and have implemented an architecture for rapid energy transfer. The perylene pentamer resulting from two design principles (increasing the number of chromophores and rapid energy transfer) is shown in Scheme 2. The acceptor is functionalized so that its absorption spectrum broadens the region of the spectrum covered by the pentamer.

As a side effect of the energy transfer design, the self-absorption of the array is reduced. If the fluorescence quantum

Special Issue: Prashant V. Kamat Festschrift

Received: January 31, 2018
Revised: February 23, 2018
Published: February 24, 2018

DOI: 10.1021/acs.jpcc.8b01084

**Scheme 1. Structure of the Monoimide Diester Donor (Top) and Tetraphenoxy Diimide Acceptor (Bottom) in Monomer Form**

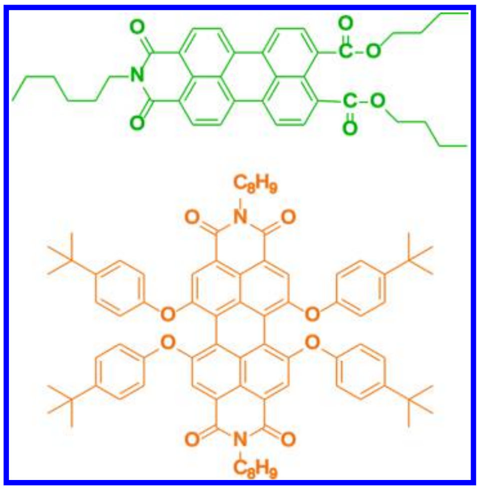

yield of this system can be increased, it may be suitable for luminescent solar concentration, a technology where fluorescence drives solar energy into a large and cheap waveguide, ultimately sending it to a small, relatively high cost solar cell.

In the absence of perfect fluorescence quantum yield, self-absorption in a device which contains concentrated fluorophores, such as a luminescent solar concentrator, can make the device inefficient.[23,24] If the fluorophore's fluorescence quantum yield is $y$, then after $n$ absorption-and-fluorescence cycles, the yield is reduced to $y^n$. As the number of cycles increases, energy is quickly lost.

## ■ EXPERIMENTAL SECTION

**Synthesis.** The synthesis methods were developed from the work of June et al.[25]

**Dimer.** Dimethylformamide (5 mL) was added to di(bromopropyl) isophthalate (40 mg, 98 μmol) and 3,4-dibutylcarboxylate-9,10-imidoperylene (170 mg, 328 μmol) with cesium carbonate (70 mg, 210 μmol). This was placed in an oil bath at 80 °C with stirring for 3 h. The reaction was then worked up by addition of aqueous hydrochloric acid (50 mL, 2 M) then filtered and air-dried. The resultant material was then purified by preparative thin layer chromatography (1% methanol in dichloromethane) to yield the dimer as a red solid (89 mg, 69 μmol, 70%).

HR-ESI: $[(C_{78}H_{68}N_2O_{16}{}^+Na)^+] = [(M^+Na)^+]$, calcd, 1311.4461; found, 1311.4463. $^1$H NMR (300 MHz, $CDCl_3$): 9.08 (1H, t, 1.6, $H_{Ar}$-isophthalic), 8.36 (2H, dd, 7.8, 1.6, $H_{Ar}$-isophthalic), 8.11 (4H, d, 8.1, $H_{Ar}$-perylene), 7.86 (4H, d, 8.0, $H_{Ar}$-perylene), 7.73 (4H, d, 8.0, $H_{Ar}$-perylene), 7.69 (4H, d, 8.1, $H_{Ar}$-perylene), 7.62 (1H, t, 7.8, $H_{Ar}$-isophthalic), 4.57 (4H, m, propyl X−$[CH_2]$−$CH_2$), 4.51 (4H, m, propyl X−$[CH_2]$−$CH_2$), 4.40 (8H, t, 6.9, butyl O−$[CH_2]$−), 2.39 (4H, br m), 1.87 (8H, q, 7.2, butyl $OCH_2$−$[CH_2]$−), 1.56 (8H, sx, 7.5, butyl $CH_2$−$[CH_2]$−$CH_3$), 1.05 (12H, t, 7.4, butyl $CH_2$−$[CH_3]$).

**Pentamer.** Tetraphenoxydi(di(bromopropyl)-imidoisophthalate)perylene: Tetra($p$-tBu-phenoxy)di(imidoisophthalic acid)perylene (1.25 g, 0.95 mmol), 1,3-dibromopropane (60 mL), and potassium carbonate (5.0 g) were combined along with water (30 mL) and placed into an oil bath at 110 °C for 3 h. Chloroform was then added to the reaction and the organic phase separated and passed through a Celite plug. The solvent was then removed and the residue

**Scheme 2. Structure of the Donating Dimer (Top) and Pentamer (Bottom)**

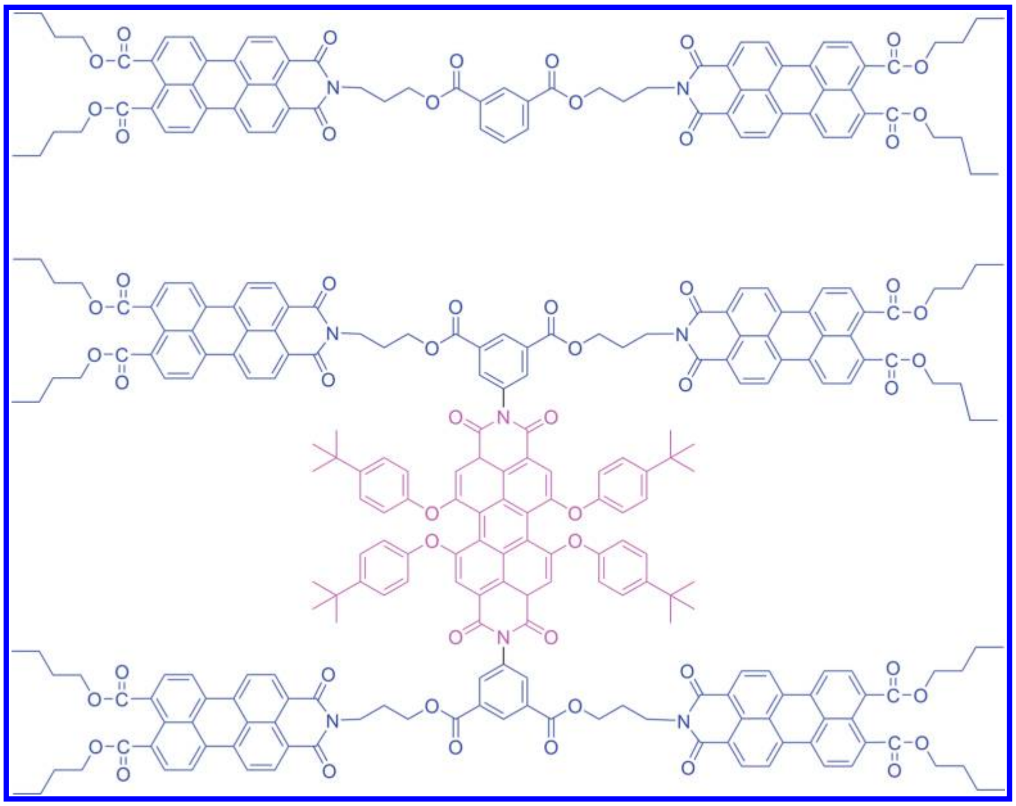

**Table 1. Quantum Yields and Self-Absorption Ratios ($S$)**

| molecule | fluorophores | excitation wavelength | quantum yield | $S$ |
|---|---|---|---|---|
| donor | 1 | 460 | 0.81(4) | 3.2 |
| acceptor | 1 | 520 | 0.78(2) | 4.8 |
| dimer | 2 | – | low | $\sim 3 \times 10^2$ |
| trimer "D-A1-D"[12] | 3 | 495 | 0.62(2) | 9 |
| pentamer | 5 | 480 | 0.54(3) | 6.0 |

purified on silica with a 300:100:1 dichloromethane:hexane:2-propanol solvent system. This produced the tetra(*p*-tBu-phenoxy)di(di(bromopropyl)imidoisphthalate)perylene as a dark blue solid (786 mg, 0.43 mmol, 45%).

$^1$H NMR (300 MHz, $CDCl_3$): 8.75 (2H, t, 1.5, $H_{Ar}$-isophthalic), 8.26 (4H, s, $H_{Ar}$-perylene), 8.13 (4H, d, 1.5, $H_{Ar}$-isophthalic), 7.24 (8H, d, $H_{Ar}$-phenoxy), 6.86 (8H, d, 8.8, $H_{Ar}$-phenoxy), 4.49 (8H, t, 6.1, O−[$CH_2$]−), 3.51 (8H, t, 6.5, Br−[$CH_2$]−), 2.31 (8H, quin, 6.3, $CH_2$−[$CH_2$]−$CH_2$), 1.27 (36H, s, [*p*-tBu]-phenoxy).

Tetra(*p*-tBu-phenoxy)di(di(bromopropyl)-imidoisophthalate)perylene (100 mg, 55.6 $\mu$mol) was combined in a sealed vial with monoimide dibutylester perylene (310 mg, 0.59 mmol) in *N*-methylpyrolidinone (20 mL) along with potassium carbonate (140 mg) and tetrabutylammonium bromide (60 mg). This was then placed into an oil bath at 120 °C for 45 min. The reaction was precipitated by the addition of methanol (30 mL) and filtered, washing the precipitate with methanol (60 mL). The solid was then recrystallized from neat toluene by addition of methanol to yield the tetra(propylimide dibutylester perylene)mono(tetra(*p*-tBu-phenoxy)di-(imidoisophthalate)perylene) as a dark red solid (147 mg, 41 $\mu$mol, 74%).

HR-ESI: [$(C_{220}H_{190}N_6O_{40}{}^+Na_2)_2{}^+$] = [$(M^+Na_2)_2{}^+$], calcd, 1801.6435; found, 1801.6432. $^1$H NMR (300 MHz, $CDCl_3$): 9.14 (2H, t, 1.5, $H_{Ar}$-isophthalic), 8.31 (4H, s, $H_{Ar}$-core perylene), 8.29 (4H, d, 1.4, $H_{Ar}$-isophthalic), 8.15 (8H, d, 8.0, $H_{Ar}$-appending perylene), 7.88 (8H, d, 8.0, $H_{Ar}$-appending perylene), 7.77 (8H, d, 8.0, $H_{Ar}$-appending perylene), 7.74 (8H, d, 8.0, $H_{Ar}$-appending perylene), 7.27 (8H, d, 9.0, $H_{Ar}$-core perylene phenoxy), 6.89 (8H, d, 9.0, $H_{Ar}$-core perylene phenoxy), 4.54 (16H, br m, O−[$CH_2$]−$CH_2$−[$CH_2$]−N), 4.40 (16H, t, 6.9, butyl O−[$CH_2$]−), 2.38 (8H, br m, $OCH_2$−[$CH_2$]−$CH_2$N), 1.87 (8H, m, butyl $OCH_2$−[$CH_2$]−), 1.29 (36H, s, phenoxy-[tBu]), 1.05 (24H, t, 7.4 Hz, butyl −[$CH_3$]).

**Steady-State Spectroscopy.** Absorption measurements were carried out using a Varian Cary 50 Bio spectrophotometer. Emission and excitation−emission spectra were recorded using a Cary Eclipse fluorimeter configured with 5 nm resolution.

Fluorescence quantum yields were measured relative to a reference.[26] The reference was prepared in ethanol. The donor was referenced to 2,3,6,7-Tetrahydro-9-(trifluoromethyl)-1*H*,5*H*,11*H*-(1)benzopyrano(6,7,8-*i*,*j*)quinolizin-11-one (Coumarin 540a). The acceptor, previously reported trimer "'D-A1-D'",[12] and pentamer were referenced to 4-(dicyanomethylene)-2-methyl-6-(4-dimethylaminostyryl)-4H-pyran (trade name DCM dye). The results at the excitation wavelengths used for quantum yield measurements are indicated in Table 1.

**Time-Resolved Fluorescence.** Time-resolved spectra were recorded using a Horiba Fluoromax time-correlated single photon counting instrument. The samples were excited using a 468 nm pulsed laser diode so that the light is primarily absorbed by the donor. The instrument response time is less than 1 ns. The spectral resolution is 10 nm or better.

The dimer time-resolved fluorescence is shown in Figure 1. The pentamer time-resolved fluorescence is shown in Figure 2.

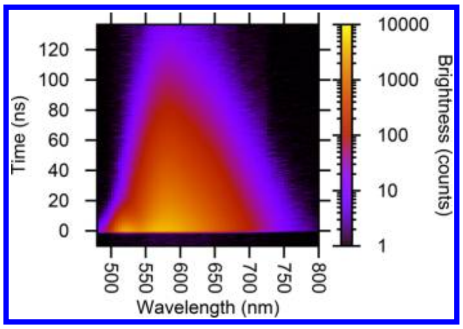

Figure 1. Time-resolved fluorescence spectrum of the dimer at a concentration of 1 $\mu$M.

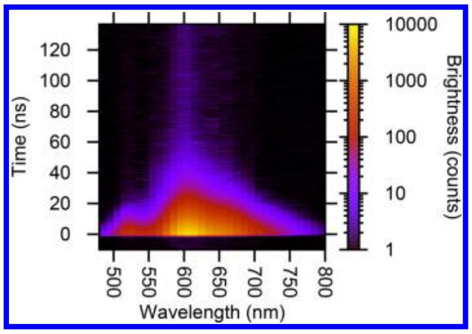

Figure 2. Time-resolved fluorescence spectrum of the pentamer, showing dynamics with only one significant linearly independent component.

**Decomposition of Time-Resolved Fluorescence.** Singular value decomposition indicated that the dimer time-resolved fluorescence included two significant linearly independent components. The pentamer time-resolved fluorescence had one component, indicating that decomposition was not required. The dimer results were decomposed using the multivariate curve resolution−alternating least squares algorithm.[27] The two-component decomposition was initialized using evolving factor analysis. As fluorescence is strictly non-negative, the model was constrained to be non-negative.

## ■ RESULTS AND DISCUSSION

**Steady State Spectra toward Energy Transfer.** As in most fluorophores, the absorption and fluorescence spectra of perylenes overlap in the region of the spectrum near the first singlet excited state. Overlap can cause self-absorption of fluorescence. In Figure 3, the overlap in the monoimide diester donor occurs in the range 500−530 nm. In the tetraphenoxy diimide acceptor, it occurs in the range 560−600 nm.

DOI: 10.1021/acs.jpcc.8b01084
*J. Phys. Chem. C* 2018, 122, 13937−13943

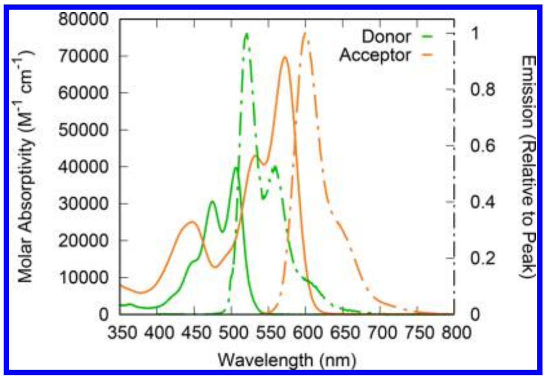

**Figure 3.** Steady-state absorption (solid lines) and emission (dashed lines) spectra of the perylene donor and acceptor monomers. The donor is excited at 500 nm. The acceptor is excited at 530 nm.

Figure 4 shows that the self-absorption of the pentamer is suppressed relative to the self-absorption of the donor alone, because the emission spectrum is offset toward longer wavelengths by about 80 nm. Meanwhile, the pentamer absorption peak is offset toward shorter wavelengths by about 100 nm relative to the acceptor.

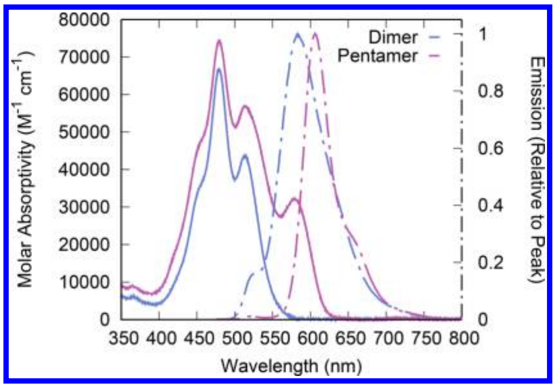

**Figure 4.** Steady-state absorption (solid lines) and emission (dashed lines) spectra of the perylene dimer and pentamer. Both molecules are excited at 450 nm, so that the acceptor is not excited. The contribution of donor monomer or dimer emission to the pentamer emission spectrum is negligible, indicating efficient energy transfer to the pentamer's acceptor. Owing to small amounts of pentamer material available, accurate concentrations could not be obtained, and thus the measured absorptivity is likely inaccurate.

In Figure 4, we find that the self-absorption of the dimer is even less than the self-absorption of the pentamer, even though the dimer lacks an acceptor to sensitize. This is caused by the dimer's tendency to form an excimer. Table 1 shows the self-absorption ratio, *S*, for each fluorophore, which is the absorption at the absorption peak divided by the absorption at the emission peak.[28]

**Excimer Formation in the Donor Dimer.** The dimer spectra are shifted relative to the donor monomer. The shift in the dimer absorption spectrum toward shorter wavelengths in Figure 4 (dark blue) as compared to Figure 3 (green) indicate H-aggregation in the dimer.

To investigate the dynamics giving rise to the substantial shift of the dimer photoluminescence spectrum about 70 nm toward longer wavelengths, we performed time-resolved fluorescence spectroscopy on each fluorophore. Figure 5 shows that the donor, acceptor, and pentamer all have similar fluorescence kinetics at 600 nm. However, the dimer fluorescence decays much more slowly. The reduced fluorescence decay rate is symptomatic of H-aggregation and subsequent excimer formation in the dimer. In an H-aggregate, the radiative transition moments of the monomers partially cancel. This leads to a slower rate of spontaneous emission and often leads to a lower fluorescence quantum yield[29] if the rate of the slowed fluorescence fails to exceed nonradiative decay rates.

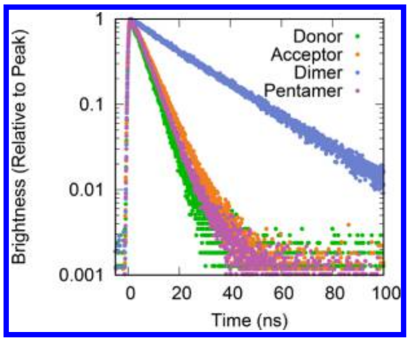

**Figure 5.** Time-resolved fluorescence of the donor, acceptor, dimer, and pentamer at 600 nm emission. The perylenes all have similar fluorescence decay rates, except the dimer (donor, $1.80(2) \times 10^8$ s$^{-1}$; acceptor, $1.40(1) \times 10^8$ s$^{-1}$; dimer, $4.434(4) \times 10^7$ s$^{-1}$; pentamer, $1.57(1) \times 10^8$ s$^{-1}$). The dimer's fluorescence lifetime is extended by H-aggregation.

Aggregation of the dimer can occur in the ground state to form an H-aggregate, or in the excited state where it forms an excimer from free monomers, one having been excited. To isolate these two kinds of aggregation, we analyzed the fluorescence decay at different wavelengths. Figure 6 shows that there are actually two rate constants present in the dimer fluorescence decay. At shorter wavelengths, the faster decay rate predominates, while at longer wavelengths the slower decay rate is most significant.

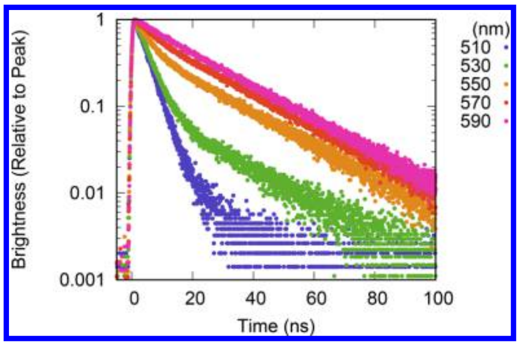

**Figure 6.** Fluorescence dynamics of the dimer at various emission wavelengths, showing the free singlet and excimer fluorescence decay rates. For emission at 510 nm, the free singlet dominates. For emission at 590 nm and greater (not shown), the excimer emission dominates. The dimer concentration is 1 $\mu$M.

Singular value decomposition indicates that there are only two significant components to the data. We used the multivariate curve resolution alternating least-squares (MCR-ALS) algorithm[27] to determine the fluorescence spectra of the two components. In Figure 7, the first component's spectrum shows two peaks. The peak near 520 nm corresponds to the donor monomer emission. It is slightly shifted to longer wavelengths owing to weak excitonic coupling to the second donor molecule in the dimer. The second peak, near 570 nm, is

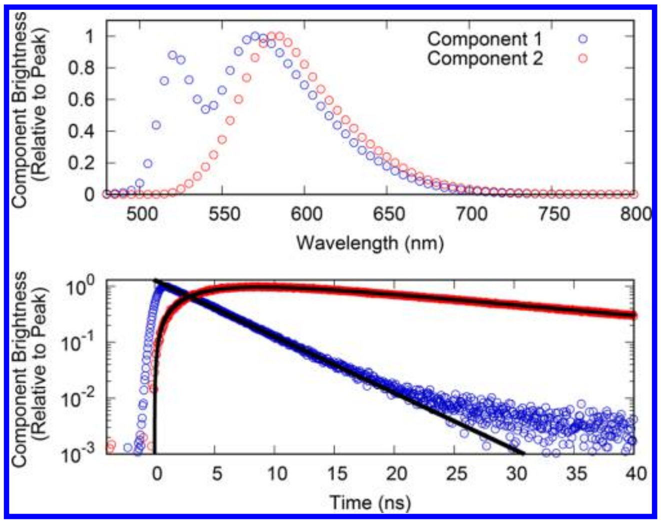

**Figure 7.** Decomposition of Figure 1, the time-resolved fluorescence of the dimer, showing conversion of the initial excited state into an excimer. The initial excited state (Component 1) includes both monomer-like and H-aggregate-like emission. The excimer (Component 2) exhibits stronger excitonic coupling than Component 1. The solid curves are our model of the excimer kinetics.

emission from dimers which are aggregated before they are excited. While these aggregated molecules presumably have a reduced fluorescence rate, their total decay rate is high because they form excimers promptly. The second component had only one peak, near 580 nm. We assign this emission to the excimer state of the dimer. The bathochromic shift of each component is smaller than the shift previously reported for a perylene dimer which was connected at both ends.[30]

The temporal profiles calculated using MCR-ALS are shown in Figure 7. The residuals, which are negligible, are displayed in Figure S1. The results indicate that the measured rise time of the first component is similar to the instrument response time and can only be interpreted as a upper bound. The second component has a longer rise time. The decay rate of the first component is equal to the rise rate of the second component, which is consistent with interconversion. This kinetic behavior is further evidence that the second component is an excimer, which forms only after the dimer is excited. Similar results have been obtained for pyrene-labeled dendrimers.[20] We modeled the two components simultaneously and concluded that the excimer formation rate is $2.323(6) \times 10^{8}\ \mathrm{s}^{-1}$. The excimer decay rate is $4.434(8) \times 10^{7}\ \mathrm{s}^{-1}$.

The excimer formation rate constant includes a contribution from radiative decay of the first MCR-ALS generated component. On the basis of the relative brightnesses of the components and the assumption that additional aggregation cannot increase quantum yield, we conclude that the excimer formation process dominates over the fluorescence. This suggests that the pre-existing aggregation effects apparent in the first component reduce its fluorescence rate relative to the monomeric donor. The resulting (unmeasurable) radiative decay rate is less than the excimer formation rate.

**Energy Transfer from the Donor to the Acceptor.** We attempted photoluminescence upconversion measurements, but did not detect any luminescence kinetics on the picosecond scale, within the (~150 fs) time-resolution of the instrument. As such, in order to demonstrate successful energy transfer from the donor to the acceptor within the pentamer, we constructed models of the excitation−emission spectra of the pentamer.

The models were built using the steady-state absorption and emission spectra of the dimer and the acceptor. In the model without energy transfer, each fluorophore's absorption spectrum was assigned to its own emission spectrum. In the model with perfect energy transfer, the absorption spectrum of the dimer and the acceptor were both assigned to the emission spectrum of the acceptor. In Figure 8, the model without energy transfer is dominated by broadband excimer emission. The model with perfect energy transfer shows the sharper emission peak of the acceptor, but with the combined excitation spectrum of the dimer and the acceptor. Our measurement of the pentamer excitation−emission spectrum is similar to the model with perfect energy transfer, and shows no evidence of

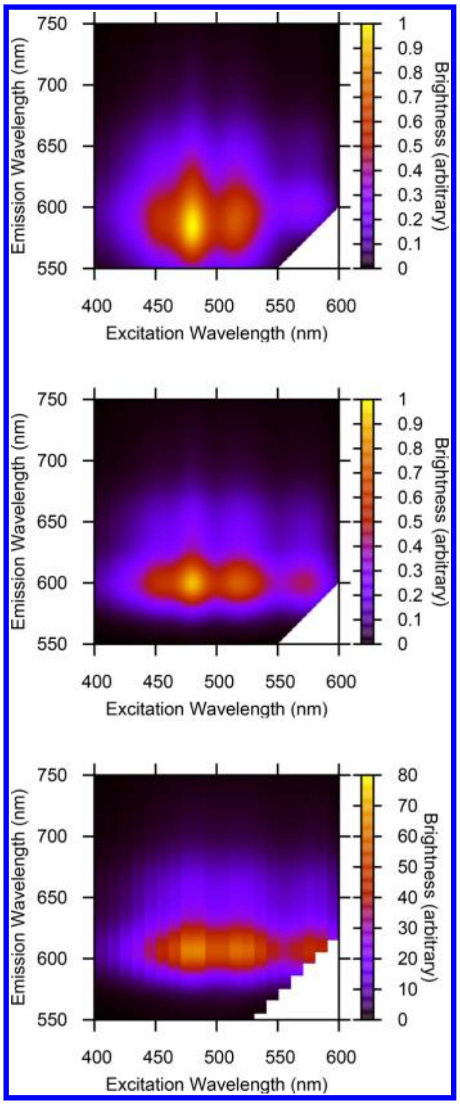

**Figure 8.** Excitation−emission spectra. Top: Model without energy transfer. Middle: Model with perfect energy transfer. Bottom: Measurement of the pentamer. The pentamer excitation−emission spectrum is consistent with perfect energy transfer. No donor emission is observed, and the excitation spectrum of the acceptor is consistent with efficient energy transfer from the donor. The white areas indicate that data is removed because the emission wavelength is similar to or shorter than the excitation wavelength.

excimer emission. We conclude that energy was successfully routed from the donor to the acceptor.

**Inhibition of Excimer Formation.** Excimer formation can function as an energy trap. In the pentamer, we find no evidence of excimers in the emission spectra, regardless of the excitation wavelength. The pentamer fluorescence decay strongly resembles the fluorescence decay of a perylene monomer. Any excimer-like kinetics are constrained to contribute less than 1% to the total fluorescence kinetics.

Singular value decomposition of the spectrally resolved fluorescence decay did not reveal a significant excimer component in the pentamer, unlike the dimer. We conclude that the reduced fluorescence quantum yield of the pentamer (Table 1) is caused by an increased nonradiative decay rate from additional vibronic coupling, not an excimer-induced reduction in the fluorescence decay rate.

We designed the pentamer to exhibit FRET,[12] where the donor emission overlaps the acceptor absorption. Overall, the evidence shows that the rapid rate of energy transfer from the donor to the acceptor exceeds that of excimer formation, even in preaggregated dimers, eliminating energy trapping.

Previous measurements of perylene donor−acceptor macromolecules[12] showed energy transfer rates of about $10^{12}$ $s^{-1}$. We found that the energy transfer rate for the pentamer was within the response time of the time correlated single photon counting instrument, and the dynamics could not be resolved by fluorescence upconversion. Therefore, we conclude that the excimer suppression is achieved with an energy transfer rate larger than $10^{12}$ $s^{-1}$.

## CONCLUSION

Upon absorption of light, the covalent perylene dimer formed an excimer, which reduced self-absorption losses. But, excimer formation suppresses the radiative decay rate, and thus is not a viable strategy for luminescence solar concentration.

By covalently linking the dimer with a perylene acceptor, we successfully traded a little self-absorption for the elimination of excimer formation. The competition between the dimer's excimer formation and energy transfer rates is summarized in Figure 9.

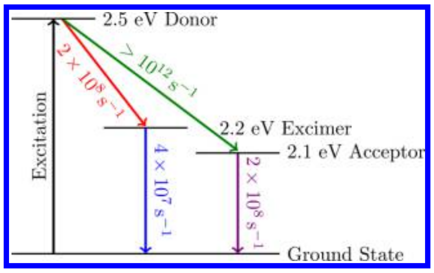

**Figure 9.** Energy levels and energy conversion rates in the pentamer. Energy transfer to the acceptor and acceptor fluorescence are the dominant processes. Not to scale.

The *tert*-butyl phenoxy groups in the bay of the acceptor shift the acceptor energy level to drive efficient energy transfer while inhibiting excimer formation between the donor and acceptor units. We have shown that energy transfer is still efficient in a five-chromophore system. Further increases in number of donor units and increased fluorescence quantum yields will enhance the usefulness of these arrays as light convertors. Our design successfully inhibits excimer formation and self-absorption.

## ASSOCIATED CONTENT

### Supporting Information

The Supporting Information is available free of charge on the ACS Publications website at DOI: 10.1021/acs.jpcc.8b01084.

Residuals of the decomposition in Figure 7 of the main text (PDF)

## AUTHOR INFORMATION

### Corresponding Author

*(T.W.S.) E-mail: timothy.schmidt@unsw.edu.au.

### ORCID

Pall Thordarson: 0000-0002-1200-8814
Timothy W. Schmidt: 0000-0001-6691-1438

### Notes

The authors declare no competing financial interest.

## ACKNOWLEDGMENTS

This work was supported by the Australian Research Council Centre of Excellence in Exciton Science (CE170100026). T.W.S. acknowledges the Australian Research Council for a Future Fellowship (FT130100177) and P.T. acknowledges the Australian Research Council for a Linkage Grant (LP130100774). This research is supported by Fluorosol Industries Pty Ltd.

## REFERENCES

(1) Perez, R.; Zweibel, K.; Hoff, T. E. Solar power generation in the US: Too expensive, or a bargain? *Energy Policy* **2011**, *39*, 7290−7297.

(2) Swallen, S.; Kopelman, R.; Moore, J.; Devadoss, C. Dendrimer photoantenna supermolecules: energetic funnels, exciton hopping and correlated excimer formation. *J. Mol. Struct.* **1999**, *485-486*, 585−597.

(3) Li, G.; Shrotriya, V.; Huang, J.; Yao, Y.; Moriarty, T.; Emery, K.; Yang, Y. High-efficiency solution processable polymer photovoltaic cells by self-organization of polymer blends. *Nat. Mater.* **2005**, *4*, 864−868.

(4) Friend, R. H.; Gymer, R. W.; Holmes, A. B.; Burroughes, J. H.; Marks, R. N.; Taliani, C.; Bradley, D. D. C.; Dos Santos, D. A.; Bredas, J. L.; Logdlund, M.; et al. Electroluminescence in conjugated polymers. *Nature* **1999**, *397*, 121−128.

(5) Baldo, M. A.; O'Brien, D. F.; You, Y.; Shoustikov, A.; Sibley, S.; Thompson, M. E.; Forrest, S. R. Highly efficient phosphorescent emission from organic electroluminescent devices. *Nature* **1998**, *395*, 151−154.

(6) Ali, M. A.; Chen, S. S.; Cavaye, H.; Smith, A. R.; Burn, P. L.; Gentle, I. R.; Meredith, P.; Shaw, P. E. Diffusion of nitroaromatic vapours into fluorescent dendrimer films for explosives detection. *Sens. Actuators, B* **2015**, *210*, 550−557.

(7) Al-Jamal, K. T.; Ruenraroengsak, P.; Hartell, N.; Florence, A. T. An intrinsically fluorescent dendrimer as a nanoprobe of cell transport. *J. Drug Targ.* **2006**, *14*, 405−412.

(8) Lee, Y.; Kim, J.; Kim, S.; Jang, W.-D.; Park, S.; Koh, W.-G. Protein-conjugated, glucose-sensitive surface using fluorescent dendrimer porphyrin. *J. Mater. Chem.* **2009**, *19*, 5643−5647.

(9) Staneva, D.; Bosch, P.; Grabchev, I. Ultrasonic synthesis and spectral characterization of a new blue fluorescent dendrimer as highly selective chemosensor for $Fe^{3+}$ cations. *J. Mol. Struct.* **2012**, *1015*, 1−5.

(10) Hasobe, T.; Kashiwagi, Y.; Absalom, M. A.; Sly, J.; Hosomizu, K.; Crossley, M. J.; Imahori, H.; Kamat, P. V.; Fukuzumi, S. Supramolecular photovoltaic cells using porphyrin dendrimers and fullerene. *Adv. Mater.* **2004**, *16*, 975−979.

(11) Chavan, S. A.; Maes, W.; Gevers, L. E.; Wahlen, J.; Vankelecom, I. F.; Jacobs, P. A.; Dehaen, W.; De Vos, D. E. Porphyrin-

Functionalized Dendrimers: Synthesis and Application as Recyclable Photocatalysts in a Nanofiltration Membrane Reactor. *Chem. - Eur. J.* **2005**, *11*, 6754−6762.

(12) Webb, J. E.; Chen, K.; Prasad, S. K.; Wojciechowski, J. P.; Falber, A.; Thordarson, P.; Hodgkiss, J. M. Quantifying highly efficient incoherent energy transfer in perylene-based multichromophore arrays. *Phys. Chem. Chem. Phys.* **2016**, *18*, 1712−1719.

(13) Maus, M.; Mitra, S.; Lor, M.; Hofkens, J.; Weil, T.; Herrmann, A.; Müllen, K.; De Schryver, F. C. Intramolecular Energy Hopping in Polyphenylene Dendrimers with an Increasing Number of Peryleneimide Chromophores. *J. Phys. Chem. A* **2001**, *105*, 3961−3966.

(14) Duhamel, J. Internal dynamics of dendritic molecules probed by pyrene excimer formation. *Polymers* **2012**, *4*, 211−239.

(15) Yip, J.; Duhamel, J.; Bahun, G. J.; Adronov, A. A study of the dynamics of the branch ends of a series of pyrene-labeled dendrimers based on pyrene excimer formation. *J. Phys. Chem. B* **2010**, *114*, 10254−10265.

(16) Swallen, S. F.; Zhu, Z.; Moore, J. S.; Kopelman, R. Correlated excimer formation and molecular rotational dynamics in phenylacetylene dendrimers. *J. Phys. Chem. B* **2000**, *104*, 3988−3995.

(17) Karni, Y.; Jordens, S.; De Belder, G.; Schweitzer, G.; Hofkens, J.; Gensch, T.; Maus, M.; De Schryver, F.; Hermann, A.; Müllen, K. Intramolecular evolution from a locally excited state to an excimer-like state in a multichromophoric dendrimer evidenced by a femtosecond fluorescence upconversion study. *Chem. Phys. Lett.* **1999**, *310*, 73−78.

(18) Lekha, P.; Prasad, E. Aggregation-Controlled Excimer Emission from Anthracene-Containing Polyamidoamine Dendrimers. *Chem. - Eur. J.* **2010**, *16*, 3699−3706.

(19) Ghaddar, T. H.; Whitesell, J. K.; Fox, M. A. Excimer formation in a naphthalene-labeled dendrimer. *J. Phys. Chem. B* **2001**, *105*, 8729−8731.

(20) Wilken, R.; Adams, J. End-group dynamics of fluorescently labeled dendrimers. *Macromol. Rapid Commun.* **1997**, *18*, 659−665.

(21) Förster, T. Zwischenmolekulare energiewanderung und fluoreszenz. *Ann. Phys.* **1948**, *437*, 55−75.

(22) Samanta, S.; Chaudhuri, D. Suppressing Excimers in H-Aggregates of Perylene Bisimide Folda-Dimer: Role of Dimer Conformation and Competing Assembly Pathways. *J. Phys. Chem. Lett.* **2017**, *8*, 3427−3432.

(23) Batchelder, J.; Zewai, A.; Cole, T. Luminescent solar concentrators. 1: Theory of operation and techniques for performance evaluation. *Appl. Opt.* **1979**, *18*, 3090−3110.

(24) Batchelder, J.; Zewail, A.; Cole, T. Luminescent solar concentrators. 2: Experimental and theoretical analysis of their possible efficiencies. *Appl. Opt.* **1981**, *20*, 3733−3754.

(25) June, S. M.; Bissel, P.; Long, T. E. Segmented block copolyesters using click chemistry. *J. Polym. Sci., Part A: Polym. Chem.* **2012**, *50*, 3797−3805.

(26) Würth, C.; Grabolle, M.; Pauli, J.; Spieles, M.; Resch-Genger, U. Relative and absolute determination of fluorescence quantum yields of transparent samples. *Nat. Protoc.* **2013**, *8*, 1535.

(27) Jaumot, J.; de Juan, A.; Tauler, R. MCR-ALS GUI 2.0: new features and applications. *Chemom. Intell. Lab. Syst.* **2015**, *140*, 1−12.

(28) Currie, M. J.; Mapel, J. K.; Heidel, T. D.; Goffri, S.; Baldo, M. A. High-efficiency organic solar concentrators for photovoltaics. *Science* **2008**, *321*, 226−228.

(29) Spano, F. C.; Silva, C. H- and J-Aggregate Behavior in Polymeric Semiconductors. *Annu. Rev. Phys. Chem.* **2014**, *65*, 477−500.

(30) Sung, J.; Nowak-Król, A.; Schlosser, F.; Fimmel, B.; Kim, W.; Kim, D.; Würthner, F. Direct Observation of Excimer-Mediated Intramolecular Electron Transfer in a Cofacially-Stacked Perylene Bisimide Pair. *J. Am. Chem. Soc.* **2016**, *138*, 9029−9032.

DOI: 10.1021/acs.jpcc.8b01084
*J. Phys. Chem. C* 2018, 122, 13937−13943